

# Atomistic Simulation Study of Striped Phase Separation in Mixed-Ligand Self-Assembled Monolayer Coated Nanoparticles

Pradip Kr. Ghorai<sup>\*,†,‡</sup> and Sharon C. Glotzer<sup>\*,‡,§</sup>

*Indian Institute of Science Education and Research - Kolkata, Mohanpur Campus-741252, Nadia, India, Department of Chemical Engineering, University of Michigan, Ann Arbor, Michigan 48109, United States, and Department of Material Science and Engineering, University of Michigan, Ann Arbor, Michigan 48109, United States*

Received: June 1, 2010; Revised Manuscript Received: October 5, 2010

Atomistic molecular dynamics simulations are performed to study the stripelike patterns formed by phase separation of immiscible surfactants grafted on spherical surfaces. In previous work (*Phys. Rev. Lett.* 2007, 99, 226106), we showed that the formation of a striped phase for a mixture of two different length surfactants does not depend on the detailed chemistry of the molecules. Rather, the pattern is stabilized by increased conformational entropy related to the geometry of the molecules. In this paper, we extend the atomistic simulations of our earlier study to investigate the dependence of stripe thickness on charges on the head groups, the relative length difference of the tail, and the strength of the repulsion between the surfactants. Previously, we studied the dependence of the tilt angle for a homoligand surfactant on a nanoparticle surface (*J. Phys. Chem. C* 2007, 111, 15857). Here, we study the dependence of the tilt angle for mixed-ligand surfactants on a spherical nanoparticle surface. We observe that the tilt angle increases with surfactant length but does not play a significant role in stripe formation.

## 1. Introduction

Self-assembled monolayers (SAMs) of surfactants adsorbed via their head groups on solid substrates have been an active area of research for over two decades.<sup>1–5</sup> Because of their stability and ease of preparation, they have served as model surfaces for a variety of studies, including, for example, corrosion prevention,<sup>6</sup> interactions of biomolecules with surfaces,<sup>7</sup> protein resistance,<sup>8</sup> molecular recognition,<sup>9</sup> and electrode modification.<sup>10</sup> SAMs on nanoparticle surfaces have recently attracted attention due to their interesting optical<sup>11</sup> and electronic<sup>12</sup> properties and potential applications in nanolithography,<sup>13</sup> bottom-up assembly,<sup>14,15</sup> catalysis,<sup>16</sup> drug delivery,<sup>17</sup> and biosensing.<sup>18</sup>

SAMs of different molecules can be formed on various solid substrates, such as gold, silver, and silicon, by spontaneous adsorption of molecules from solution.<sup>19</sup> Alkanethiol SAMs on the Au(111) surface are the most widely studied because gold can be handled in ambient conditions. SAMs of hydrocarbon chains are the simplest ideal model system of biological membranes and biocompatible materials.<sup>20,21</sup> Recently, monolayer-protected metal nanoparticles (NPs) have found use in a variety of fields<sup>22–27</sup> due to their unique electronic and optical properties. The ligand shell that forms a protecting monolayer (alkanethiol SAM) around the NPs provides a range of interesting properties, for example, solubility in many solvents,<sup>28</sup> electron-transfer efficiency,<sup>29</sup> electrochemical charging,<sup>30</sup> sensing of biomolecules,<sup>26</sup> etc. In 2004, Jackson et al. coadsorbed two different surfactants on gold nanoparticles to obtain a mixed SAM that not only demonstrated an interesting striped phase

separation but is also potentially useful in protein inhibition and catalysis<sup>31</sup> due to the nanoscale width of the stripes.<sup>32–35</sup>

In our earlier study,<sup>33</sup> we reproduced using atomistic MD simulations the striped patterns observed in the Jackson et al. experiments.<sup>32</sup> Using dissipative particle dynamics (DPD) simulations, we demonstrated that striped phase separation will occur when one of the adsorbing surfactants is sufficiently longer and/or bulkier than the other. We showed this to be the case for immiscible mixtures of surfactants on flat surfaces as well, again, provided the difference in length or tail bulkiness is sufficient. We also explained that the gain of conformational entropy of the longer or bulkier chains at an interface resulted in a lower free energy than can be achieved from complete demixing, resulting in microphase-separated stripes of 50:50 mixtures. In this paper, we present in section 3.1 results of detailed atomistic molecular dynamics simulations for different immiscible surfactant mixtures on spherical nanoparticle surfaces that we performed to further test our earlier explanation of the origin of striped phase formation. In section 3.2, we show how the stripe thickness depends on various external parameters, such as the relative length difference between the surfactants and the strength and range of repulsion between unlike surfactants as well as long-range electrostatic interaction. In section 3.3, we investigate how the tilt angle of mixed-ligand surfactants on a spherical NP surface depends on those parameters. We observe that the average tilt angle of alkanethiols on NP surfaces is large as compared with that on flat substrates and small as compared with that for homoligand alkanethiols on a spherical NP surface. We also find that the tilt angle of the surfactants does not play a significant role in the formation of stripes.

\* To whom correspondence should be addressed. E-mail: sglotzer@umich.edu (S.C.G.), pradip@iiserkol.ac.in (P.K.G.).

† Indian Institute of Science Education and Research.

‡ Department of Chemical Engineering, University of Michigan.

§ Department of Material Science and Engineering, University of Michigan.

## 2. Methodology

**2.1. Model and Simulation Details.** The total energy ( $V_{\text{total}}$ ) of an alkanethiol chain is given by

$$V_{\text{total}} = V_{\text{intra}} + V_{\text{inter}} \quad (1)$$

Here,  $V_{\text{intra}}$  represents the bonded interactions that arise from bond stretching ( $V_{\text{bond}}$ ), bond bending ( $V_{\text{angle}}$ ), and torsion ( $V_{\text{dihedral}}$ )

$$V_{\text{intra}} = V_{\text{bond}} + V_{\text{angle}} + V_{\text{dihedral}} \quad (2)$$

where

$$V_{\text{bond}} = \sum_{ij} K_{ij}^r (r_{ij} - r_{ij}^{\text{eq}})^2 \quad (3)$$

$$V_{\text{angle}} = \sum_{ijk} K_{ijk}^\theta (\theta_{ijk} - \theta_{ijk}^{\text{eq}})^2 \quad (4)$$

and

$$V_{\text{dihedral}} = \sum_{ijkl} a_1 (1 + \cos(\phi_{ijkl})) + a_2 (1 + \cos(2\phi_{ijkl})) + a_3 (1 + \cos(3\phi_{ijkl})) \quad (5)$$

Here,  $r_{ij}$  is the bond distance between two atoms  $i$  and  $j$  and  $r_{ij}^{\text{eq}}$  is the equilibrium bond length.  $\theta_{ijk}$  defines the angle between three atoms,  $i$ ,  $j$ , and  $k$ , and  $\theta_{ijk}^{\text{eq}}$  is the equilibrium angle. The four atoms,  $i$ ,  $j$ ,  $k$ , and  $l$ , define a dihedral angle  $\phi_{ijkl}$ .  $K_{ij}^r$ ,  $K_{ijk}^\theta$ ,  $a_1$ ,  $a_2$ , and  $a_3$  are constants.

$V_{\text{inter}}$  is the nonbonded interaction that we model in terms of a short-range 6–12 Lennard-Jones (LJ) potential for head–head, head–tail, and tail–tail interactions for like surfactants. Nonbonded interactions between atoms or groups of atoms on unlike surfactants are modeled via the Buckingham potential without the attractive component ( $U(r) = 500 e^{r/0.4}$ , where  $r$  is the distance between unlike atoms or groups of atoms). The pairwise additive Morse potential is used for the interaction between sulfur and gold atoms.<sup>36</sup> The LJ pair potential is defined by

$$V_{\text{inter}} = \sum_{ij} 4\epsilon_{ij} \left[ \left( \frac{\sigma_{ij}}{r_{ij}} \right)^{12} - \left( \frac{\sigma_{ij}}{r_{ij}} \right)^6 \right] \quad (6)$$

where  $\sigma_{ij}$ ,  $\epsilon_{ij}$ , and  $r_{ij}$  are, respectively, the atomic diameter, well depth, and distance between two interacting atoms  $i$  and  $j$ . The LJ potential is truncated and shifted smoothly to zero at a cutoff radius of  $r_c$ :

$$V_{\text{inter}}(r) = V_{\text{inter}}(r) - V_{\text{inter}}(r_c) - (r - r_c) \frac{dV_{\text{inter}}}{dr} \Big|_{r=r_c} \quad (7)$$

The Morse potential is defined by

$$V_{\text{Morse}}^{\text{Au-S}} = D_e [(1 - \exp(-\alpha(r - r_e)))^2 - 1] \quad (8)$$

where  $r$  is the distance between surface Au atoms and sulfur head groups and  $D_e$ ,  $r_e$ , and  $\alpha$  are empirical parameters.<sup>36</sup> All the interaction parameters used in our simulations are listed elsewhere.<sup>33,37</sup> We use the Lorentz–Berthelot combination rules<sup>38</sup> for the cross-interaction parameters.

We perform MD simulations in the canonical ensemble (constant number of ligands  $N$ , volume  $V$ , and temperature  $T$ ) for SAMs of alkanethiols adsorbed on a surface of a single gold nanosphere with a diameter of 7 nm. Experimentally, it was found that, in the case of alkanethiol-based SAMs on a Au(111) surface, the sulfur head groups form a  $(\sqrt{3} \times \sqrt{3})R30^\circ$  two-dimensional triangular lattice with a surface density of  $21.6 \text{ \AA}^2$  per chain.<sup>39</sup> We use this surface density in our simulations. We use a 1:1 molar composition of  $\text{SH}-(\text{CH}_2)_m-\text{COOH}$  and  $\text{SH}-(\text{CH}_2)_n-\text{CH}_3$ , where  $m$  varies from 2 to 20 and  $n$  varies from 7 to 18. We use the united atom model for the  $\text{CH}_2$ ,  $\text{CH}_3$ , and  $\text{OH}$  groups and a cutoff radius of  $10 \text{ \AA}$  for the nonbonded interactions between atoms or groups of atoms on the same type of surfactants. For the repulsive potential between atoms or groups of atoms on unlike surfactants, we use a cutoff radius of  $\sigma_s$ , the collision diameter. The distance between the gold surface and the sulfur headgroup ( $d_{\text{Au-S}}$ ) of the alkanethiol is fixed at  $2.38 \text{ \AA}$  throughout the simulations.<sup>40</sup> Other details specific to certain systems will be mentioned while discussing their results. To study the effect of long-range interactions on stripe formation, we put equal, but opposite, charges on surfactant head groups. The details of the headgroup charges and other related parameters are discussed in section 3.2.3. All simulations are carried out using a slightly modified version of the DL\_POLY molecular simulation package.<sup>41</sup> We use a Nose–Hoover thermostat to keep the system temperature constant at any desired temperature throughout the simulations. We use an integration time step of 2.0 fs, which yields good conservation of energy and linear momentum. Equilibration of the SAMs is performed over a duration of 10 ns. Different properties are computed from configurations stored at an interval of 10 ps from a production run of 10 ns.

**2.2. Initialization.** To model the gold NPs, Au atoms are initially assigned in a random close-packed configuration on the surface of a sphere at a surface density of  $10.4 \text{ \AA}^2/\text{Au atom}$ . We then relax the system at 0 K to optimize the initial structures. The carbon chains are initialized in the trans configuration, perpendicular to the surface with their sulfur head groups distributed randomly on the surface. The backbone planes of the molecules are also randomly oriented. All atoms are assigned random initial velocities according to the Maxwell–Boltzmann distribution corresponding to the target temperature. We then run the system for 10 ns until it equilibrates and the chains adopt an equilibrated tilt angle. In these studies, we define the tilt angle as follows. On a spherical surface, the tilt angle is defined as the angle between two vectors: (i) a vector connecting the sulfur head group and the odd carbons of the alkane chain and (ii) a vector perpendicular to the surface of the sphere and passing through the sulfur headgroup (Figure 1). The tilt angle reported for a given choice of surfactant here is computed by averaging over all time steps and odd carbons.

### 3. Results and Discussion

The model and force field parameters used here were validated previously<sup>33</sup> on a Au(111) surface against the experimentally known tilt angle of the molecule. The results discussed elsewhere<sup>37</sup> confirm the validity of the model and force fields to be used in our subsequent study.

**3.1. Structures of SAMs.** In our previous study,<sup>33</sup> we reported first the results of atomistic simulations showing stripes for mixtures of (i)  $\text{SH}-(\text{CH}_2)_3-\text{CH}_3$  and  $\text{SH}-(\text{CH}_2)_5-\text{CH}_3$ , (ii)  $\text{SH}-(\text{CH}_2)_{10}-\text{COOH}$  and  $\text{SH}-(\text{CH}_2)_{11}-\text{CH}_3$ , and (iii)  $\text{SH}-(\text{CH}_2)_2-\text{COOH}$  and  $\text{SH}-(\text{CH}_2)_2-\text{CH}_3$ . Figure 2 shows snapshots of the equilibrium structures from atomistic simulation

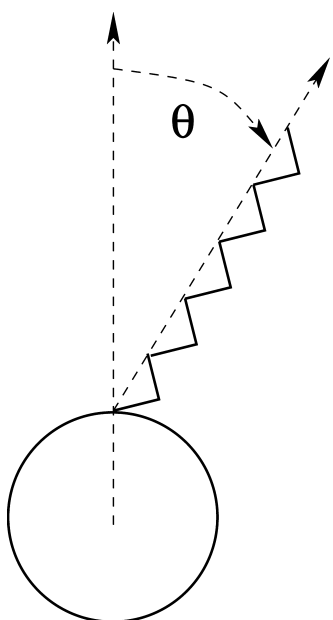


**Figure 1.** Schematic representation of the tilt angle ( $\theta$ ) for an alkanethiol on a spherical nanoparticle surface.

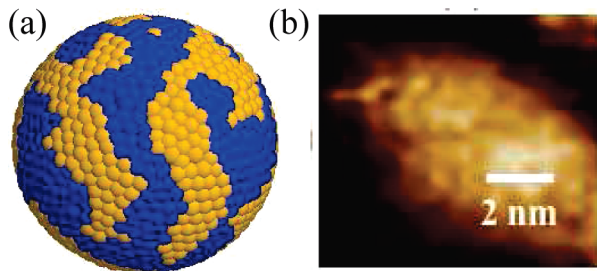


**Figure 2.**  $\text{SH}-(\text{CH}_2)_2-\text{COOH}:\text{SH}-(\text{CH}_2)_7-\text{CH}_3$  surfactant mixture of SAMs from (a) atomistic simulation and (b) experiment.<sup>32</sup>

and experiment of two unequal length surfactants,  $\text{SH}-(\text{CH}_2)_2-\text{COOH}$  and  $\text{SH}-(\text{CH}_2)_7-\text{CH}_3$  at 360 K on a sphere with a diameter of 7 nm reproduced from ref 32. To determine if the striped pattern on an NP surface is system-specific, we simulate different pairs of immiscible surfactants. First, as in an earlier experiment,<sup>32</sup> we simulate the short surfactants with carboxyl tail groups and the long surfactants with methyl tail groups. Next we interchange the tail groups, that is, the methyl group for the short surfactant and the carboxyl group for the long surfactant, and finally, we simulate both surfactants with the same methyl tail group. We observe stripes as the equilibrium phase in all cases (Figure 3a–c), demonstrating that the formation of stripes for two immiscible surfactants of sufficiently different lengths is universal and does not depend on the chemistry of the surfactants. This confirms our earlier conclusion based on DPD simulations only.<sup>33</sup>

In recent experiments<sup>32</sup> and simulations,<sup>33</sup> it was found that a mixture of two surfactants,  $\text{SH}-(\text{CH}_2)_{10}-\text{COOH}$  and  $\text{SH}-(\text{CH}_2)_{11}-\text{CH}_3$ , of almost equal length also forms stripes. In contrast, we predicted that a mixture of two very short surfactants of equal length, namely,  $\text{SH}-(\text{CH}_2)_2-\text{COOH}$  and  $\text{SH}-(\text{CH}_2)_2-\text{CH}_3$ , shows bulk phase separation into a Janus particle,<sup>42</sup> as shown in Figure 4. We performed simulations of these two surfactants for lengths that varied between these two limits and find that stripes form and sharpen as the tail lengths increase beyond three  $\text{CH}_2$  groups. These results support our argument, based on our previous mesoscale simulations, that stripes form only when sufficient conformational entropy is

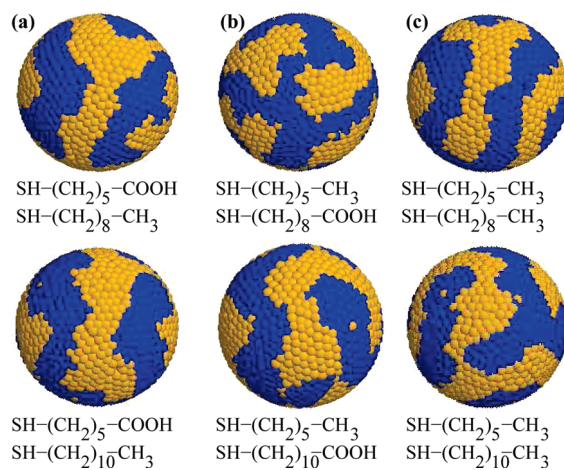


**Figure 3.** Snapshots of the SAMs for different surfactant mixtures of surfactants: (a) bulky carboxyl group is on the short surfactant, (b) bulky carboxyl group is on the long surfactant, and (c) both the tail ends have the same methyl group. The dark (blue) and light (yellow) beads are head groups of surfactants that are short and long, respectively.

gained by their formation so as to result in a lower free energy than would be obtained from bulk separation. Here, that entropic gain arises from an increased free volume for the bulkier tail end groups ( $\text{SH}-(\text{CH}_2)_{10}-\text{COOH}$  has a bulkier tail end group as compared with  $\text{SH}-(\text{CH}_2)_{10}-\text{CH}_3$ ). During the stripe formation, the entropy of the system decreases as we know that entropy decreases during the mixing of two different pure components. For two different length surfactants on a curved surface, the gain of entropy for the long surfactant is large due to availability of ample free volume around the surfactant tail group. This entropy gain overcomes the loss of entropy due to stripe formation.

**3.2. Stripe Thickness.** We next investigate the model parameters that control stripe thickness. Our studies show that the stripe thickness depends on various factors, such as the solvent, the length of the alkanethiol tail, charge on the headgroup, and other factors, as investigated below.

**3.2.1. Relative Length Difference ( $\Delta l$ ).** Our results in section 3.1 of two almost equal length ( $\Delta l \approx 0$ ) surfactants showed that the surfactant tail length is significant in controlling the stripe thickness.<sup>33</sup> In Figure 5, we show the variation of stripe thickness when the length difference between the surfactants is nonzero ( $\Delta l = 5$ ) for a repulsion strength and range discussed in section 2.1. Even for  $\Delta l \neq 0$ , we observe a similar dependence of stripe thickness on surfactant tail length. When both the surfactants are short, the stripe thickness decreases rapidly with surfactant length. Beyond a certain length however, there is no variation of stripe thickness with further increase in surfactant length. Though length differences are the same (five  $\text{CH}_2$  groups) for all the systems, the gain of entropy is more for the long surfactant because the availability of free volume for the surfactant tail increases with surfactant length. Hence, the stripe thickness decreases with surfactant length. Beyond a certain length, the stripe thickness is very thin and a further gain of entropy due to the increase in surfactant length does not have any effect on stripe thickness. Thus, we conclude that surfactant length is more important than length difference in controlling the stripe thickness for any interaction strength.

**3.2.2. Repulsion Strength and Range of Repulsion.** Through a change in solvent, it is possible to effect a change in the immiscibility between the two ligands. This can be modeled by tuning both the range and the strength of the repulsive

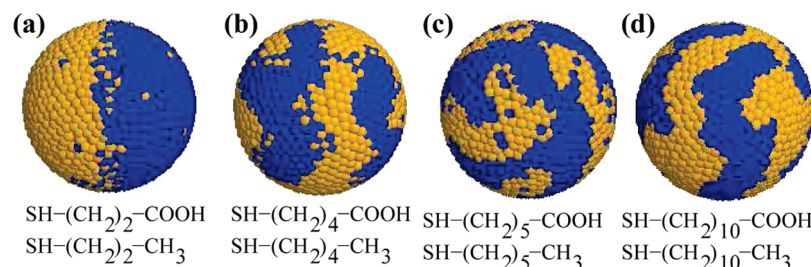


**Figure 4.** Snapshots of the SAMs for two approximately equal length surfactants with increasing tail lengths. Both the surfactants have (a) 2  $\text{CH}_2$  groups, (b) 4  $\text{CH}_2$  groups, (c) 5  $\text{CH}_2$  groups, and (d) 10  $\text{CH}_2$  groups.

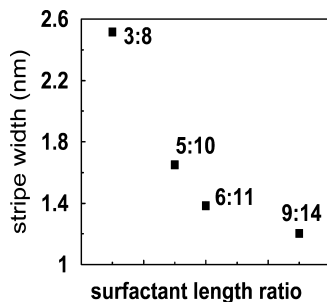


**Figure 5.** Variation of stripe width as a function of surfactant length for a mixture of  $\text{SH}-(\text{CH}_2)_m-\text{COOH}$  and  $\text{SH}-(\text{CH}_2)_n-\text{CH}_3$ , where  $m$  varies from 3 to 9 and  $n$  varies from 8 to 14. The length difference ( $\Delta l = 5 \text{ CH}_2$  groups) is fixed.

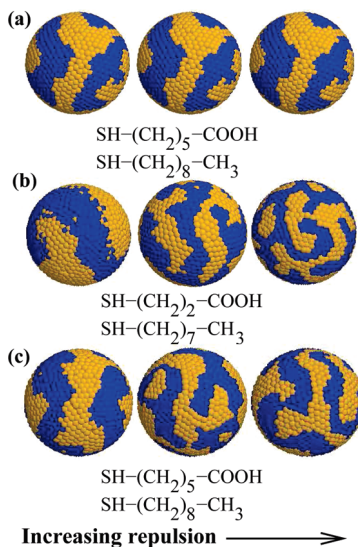


**Figure 6.** Snapshots of the SAMs for three different surfactant mixtures with increasing repulsion between the unlike surfactants: (a) mixture of  $\text{SH}-(\text{CH}_2)_5-\text{COOH}$  and  $\text{SH}-(\text{CH}_2)_8-\text{CH}_3$ , where the range of repulsion is equal to the collision diameters of the interaction sites, (b) mixture of  $\text{SH}-(\text{CH}_2)_2-\text{COOH}$  and  $\text{SH}-(\text{CH}_2)_7-\text{CH}_3$ , and (c)  $\text{SH}-(\text{CH}_2)_5-\text{COOH}$  and  $\text{SH}-(\text{CH}_2)_8-\text{CH}_3$ , where the range of repulsion is 14 Å.

interaction between the two ligand types. We varied the interaction range from  $\sigma_s$  (collision diameter) to 14 Å and the strength by a factor of 8; the results are summarized in Figure 6. When the range of repulsion between the interaction sites of the unlike surfactants is very short and equal to their collision diameter, we do not observe any significant dependence of stripe thickness on repulsion strength (Figure 6a). However, when the range of repulsion between the interaction sites is 14 Å much larger than the collision diameter (Figure 6b, c), we observe that the stripe thickness decreases with increasing repulsion strength by a factor of 4 and 8. If the range of repulsion between the interaction sites is very short, the increase of repulsion

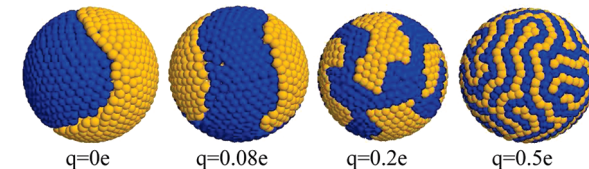


**Figure 7.** Variation of stripe width for different head group charges for a 1:1 mixture of two different types of surfactants. The surfactants contain equal, but opposite, head group charges.

strength does not have any effect on their mutual interactions because one surfactant cannot see its nearest neighbor. But when the range of repulsion is more, the increase in repulsion strength has a significant effect on their mutual interactions.

In the case of an experiment, a change in solvent changes the immiscibility between the surfactants. This effect can be considered by changing the repulsion strength and range of repulsion between the surfactants. By changing the pH of a system, more negative charge is induced on thiol head groups. Hence, repulsion between the surfactant will increase due to the increase in pH. Thus, it should be possible to obtain stripes of different thicknesses by the judicious choice of solvent or by reducing the salt pH.

**3.2.3. Electrostatic Interactions.** We expect that long-range electrostatic interaction between the surfactant head groups should play a significant role both in stabilizing the stripes and in controlling their thickness. Earlier studies showed that the self-assembly of cationic–anionic incompatible mixtures on flat and cylindrical surfaces form microphase separated structures.<sup>43–45</sup> The structures of the equilibrium phases largely depend on the charge ratio, that is, on the strength of the long-range attraction between unlike charges and the repulsion between like charges.<sup>43–45</sup> Mathematically, the role of charge in modifying bulk phase separation is identical to the role of polymeric constraints in block copolymers and chemical reactions in reacting, immiscible mixtures. These studies all indicate the important role of long-range, effectively repulsive interactions in stabilizing microphase separated structures.

In this study, we use two identical, but immiscible, model surfactants. We consider 50% of the surfactant as type I, whose head groups are positively charged, and the other 50% as type II, whose head groups are negatively charged. The interaction parameters between the surfactants are identical with respect to the choice of alkanethiol, but the mass of the atoms and the repulsion strength between the unlike surfactants are chosen so that they form a completely phase-separated structure for zero headgroup charges (Figure 7). Because the lengths of the two surfactant types are equal and there is no bulky head group on either type, there is no conformational entropic gain from forming stripes.<sup>32,33</sup> However, the charge on the head group increases, stripes emerge<sup>33</sup> as expected, and the stripe thickness decreases significantly with increasing charge magnitude. Thus, electrostatic interactions can be used to enhance stripe formations.

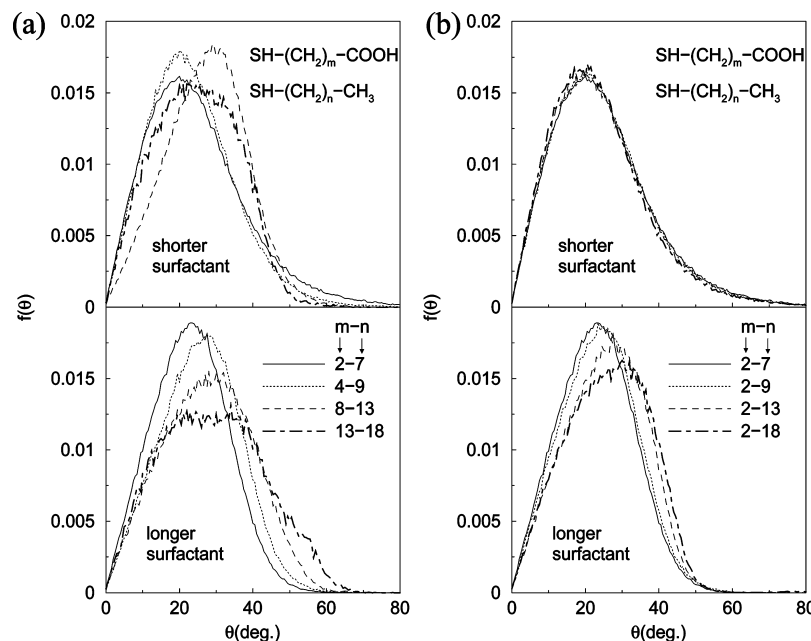


**Figure 8.** Distributions of tilt angles for mixtures of two unequal length surfactants as (a) both tail lengths increase to keep  $\Delta l = \text{constant}$  and (b) only the longer tail increases so that  $\Delta l \neq \text{constant}$ .

**3.3. Tilt Angle.** Alkanethiols are known to tilt when adsorbed onto a surface. There are several studies of the tilted structures of alkanethiol SAMs on flat gold surfaces.<sup>1,2,46</sup> In an earlier study, we investigated the tilt angle for homoligand surfactants on gold nanoparticle surfaces.<sup>37</sup> Here, we present the tilt angle for mixed-ligand surfactants on a spherical surface, compare with our previous findings for homoligands, and ascertain the effect of tilt angle on stripe formation.

**3.3.1. Effect of Molecular Length on Tilt Angle.** We compute the tilt angle for mixed-ligand SAMs on a spherical NP surface with a diameter of 7 nm at 300 K for different sets of molecules. Figure 8a, b shows the tilt angle probability distributions for short and long surfactants for two different cases. In case 1, the relative length difference  $\Delta l$  between the surfactants is fixed; in case 2, the length of the short surfactant is fixed, whereas the length of the long surfactant increases, so that  $\Delta l$  varies. In both cases, we observe that the average tilt angle for the longer surfactant is between 4° and 5° larger than that of the shorter surfactant. For  $\Delta l \neq 0$ , the extra space available for the tail of the longer surfactant<sup>33</sup> allows the molecule to adopt a larger tilt angle than for  $\Delta l = 0$  or than in the homoligand case. On a spherical surface, we find the tilt angle of the long surfactant is always greater than that of the short surfactant.

**3.3.2. Temperature Dependence.** Figure 9 shows the variation of tilt angle for mixed-ligand ( $m = 4$  and  $n = 9$ ) SAMs at three different temperatures on an NP surface with a diameter of 7 nm. The average tilt angles for both ligands are almost equal at very high temperature (e.g., at 900 K). As the temperature decreases, the tilt angles for both surfactants increase, but the increase is larger for the longer surfactant than for the shorter surfactant, as expected from the finding in section 3.3.1. This is, again, due to the lack of available space for the short surfactant to tilt appreciably.

**3.3.3. Effect of Tilt Angle on the Formation of Stripes.** An earlier experimental study indicated that the tilt angle of the surfactant on a spherical surface may have some effect on the formation of striped microphase separation.<sup>32</sup> To test this, we initially place all the surfactants perpendicular to the surface and treat them as rigid to minimize the tilt angle. Throughout

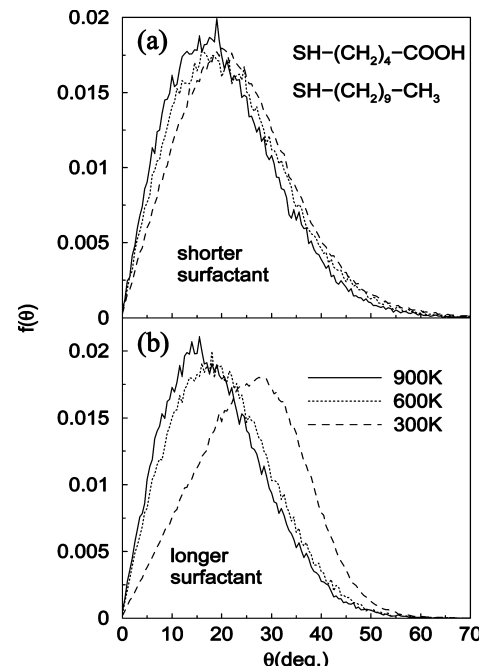


**Figure 9.** Distributions of tilt angle for a 1:1 mixture of  $\text{SH}-(\text{CH}_2)_4-\text{COOH}$  and  $\text{SH}-(\text{CH}_2)_9-\text{CH}_3$  surfactants at three different temperatures.

the simulation, we do not allow the surfactants to tilt with respect to the surface normal but instead allow them to move around the NP surface, keeping a zero tilt angle. We find that the 1:1 mixture of two unequal length surfactants (Figure 10a) and two almost equal length surfactants (Figure 10b) forms stripes with approximately the same stripe thickness as we observe when the surfactants are allowed to tilt freely on the surfaces. Our results, therefore, demonstrate that the tilt angle is not required to form stripes on NP surfaces and, in fact, has little effect on stripe width, as can be seen by comparing the image in Figure 10b with those in Figures 3c and 4c. Anecdotally, we do find that, in the systems where tilt is allowed, the phase separation occurs approximately 4 times faster.

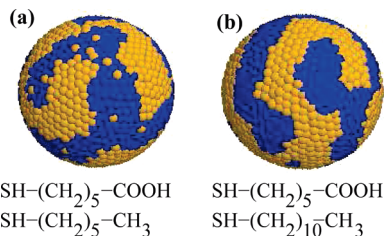


**Figure 10.** Snapshots of two different mixtures: (a) equal length and (b) unequal length. The tilt angle of surfactants on the spherical surface is kept at approximately zero throughout the simulations.

#### **4. Conclusions**

Atomistic molecular dynamics simulations of mixed-ligand surfactant SAMs have been carried out using a united-atom model to investigate the molecular packing of surfactants on a NP surface. Our studies confirm our earlier finding<sup>33</sup> that the formation of equilibrium stripe patterns does not depend on the chemical compositions of the surfactants but depends on their geometry. Our studies show that the stripe thickness depends on various factors, such as the length of the individual surfactants, length difference between the surfactants, the repulsion strength, and range of repulsion, and can be enhanced by long-range electrostatic interaction. We also studied the dependence of tilt angle for mixed-ligand surfactants on a spherical NP surface. At high temperature, the tilt angles of both the long and the short surfactants are almost equal, but at low temperature, the long surfactant is more tilted than the short surfactant. We find that the mixture of two surfactants forms stripes even for zero tilt angle. This indicates that the tilting of the surfactants on a spherical NP surface is not required for stripe formation. Our results suggest possible design strategies for obtaining stripes of different thicknesses on spherical NPs.

**Acknowledgment.** We acknowledge the National Science Foundation (CTS-2004-0679-01) for financial support. We thank F. Stellacci and A. M. Jackson for helpful discussions regarding their experiments. P.K.G. would like to thank IISER-Kolkata for the computational facility.

## References and Notes

- Figure 10.** Snapshots of two different mixtures: (a) equal length and (b) unequal length. The tilt angle of surfactants on the spherical surface is kept at approximately zero throughout the simulations.

## 4. Conclusions

Atomistic molecular dynamics simulations of mixed-ligand surfactant SAMs have been carried out using a united-atom model to investigate the molecular packing of surfactants on a NP surface. Our studies confirm our earlier finding<sup>33</sup> that the formation of equilibrium stripe patterns does not depend on the chemical compositions of the surfactants but depends on their geometry. Our studies show that the stripe thickness depends on various factors, such as the length of the individual surfactants, length difference between the surfactants, the repulsion strength, and range of repulsion, and can be enhanced by long-range electrostatic interaction. We also studied the dependence of tilt angle for mixed-ligand surfactants on a spherical NP surface. At high temperature, the tilt angles of both the long and the short surfactants are almost equal, but at low temperature, the long surfactant is more tilted than the short surfactant. We find that the mixture of two surfactants forms stripes even for zero tilt angle. This indicates that the tilting of the surfactants on a spherical NP surface is not required for stripe formation. Our results suggest possible design strategies for obtaining stripes of different thicknesses on spherical NPs.

**Acknowledgment.** We acknowledge the National Science Foundation (CTS-2004-0679-01) for financial support. We thank F. Stellacci and A. M. Jackson for helpful discussions regarding their experiments. P.K.G. would like to thank IISER-Kolkata for the computational facility.

## References and Notes

  - (1) Porter, M. D.; Bright, T. B.; Allara, D. L.; Chidsey, C. E. D. *J. Am. Chem. Soc.* **1987**, *109*, 3559.
  - (2) Nuzzo, R. G.; Dubois, L. H.; Allara, D. L. *J. Am. Chem. Soc.* **1990**, *112*, 558.
  - (3) Whitesides, G. M.; Laibinis, P. E. *Langmuir* **1990**, *6*, 87.
  - (4) Dubois, L. H.; Zegarski, B. R.; Nuzzo, R. G. *J. Am. Chem. Soc.* **1990**, *112*, 570.
  - (5) Evans, S. D.; Sharma, R.; Ulman, A. *Langmuir* **1991**, *7*, 156.
  - (6) Laibinis, P. E.; Whitesides, G. M. *J. Am. Chem. Soc.* **1992**, *114*, 9022–9028.
  - (7) Mrksich, M.; Whitesides, G. M. *Annu. Rev. Biophys. Biomol. Struct.* **1996**, *25*, 55–78.
  - (8) Harder, P.; Grunze, M.; Dahint, R.; Whitesides, G. M.; Laibinis, P. E. *J. Phys. Chem. B* **1998**, *102*, 426–436.
  - (9) Ostuni, E.; Yan, L.; Whitesides, G. M. *Colloids Surf., B* **1999**, *15*, 3–30.
  - (10) Fendler, J. H. *Chem. Mater.* **2001**, *13*, 3196–3210.
  - (11) Malinsky, M. D.; Kelly, K. L.; Schatz, G. C.; Van Duyne, R. P. *J. Am. Chem. Soc.* **2001**, *123*, 1471–1482.
  - (12) Chen, S. W.; Murray, R. W.; Feldberg, S. W. *J. Phys. Chem. B* **1998**, *102*, 9898–9907.
  - (13) Malinsky, M. D.; Kelly, K. L.; Schatz, G. C.; Van Duyne, R. P. *J. Phys. Chem. B* **2001**, *105*, 2343–2350.
  - (14) Boal, A. K.; Ilhan, F.; DeRouchey, J. E.; Thurn-Albrecht, T.; Russell, T. P.; Rotello, V. M. *Nature* **2000**, *404*, 746–748.
  - (15) DeVries, G. A.; Brunnbauer, M.; Hu, Y.; Jackson, A. M.; Long, B.; Neltner, B. T.; Uzun, O.; Wunsch, B. H.; Stellacci, F. *Science* **2007**, *315*, 358–361.
  - (16) Pasquato, L.; Rancan, F.; Scrimin, P.; Mancin, F.; Frigeri, C. *Chem. Commun.* **2000**, 2253–2254.
  - (17) Han, G.; Ghosh, P.; Rotello, V. M. *Nanomedicine* **2007**, *2*, 113–123.
  - (18) Merkoci, A. *FEBS J.* **2007**, *274*, 310–316.
  - (19) Ulman, A. *An Introduction to Ultra-Thin Organic Films: From Langmuir-Blodgett to Self-Assembly*; Academic Press, Inc: San Diego, CA, 1991.
  - (20) Collinson, M.; Bowden, E. F.; Taylor, M. J. *Langmuir* **1992**, *8*, 1247.
  - (21) Haussling, L.; Ringsdorf, H.; Schmitt, F. J.; Knoll, W. *Langmuir* **1991**, *7*, 1837.
  - (22) Shevchenko, E. V.; Talapin, D. V.; Kotov, N. A.; O'Brien, S.; Murray, B. C. *Nature* **2006**, *439*, 55.
  - (23) Andres, R. P.; Bielefeld, J. D.; Henderson, J. I.; Janes, D. B.; Kolagunta, V. R.; Kubik, C. P.; Mahoney, W. J.; Osifchim, R. G. *Science* **1996**, *273*, 1690.
  - (24) Chen, S. W.; Ingram, R. S.; Hostetler, M. J.; Pietron, J. J.; Murray, R. W.; Schaaff, T. G.; Khouri, J. T.; Alvarez, M. M.; Whetten, R. L. *Science* **1998**, *280*, 2098.
  - (25) Fick, J. F.; Zamborini, F. P.; Osisek, A.; Murray, R. W. *J. Am. Chem. Soc.* **2001**, *123*, 7048.
  - (26) You, C. C.; De, M.; Han, G.; Rotello, V. M. *J. Am. Chem. Soc.* **2005**, *127*, 12873.
  - (27) You, C. C.; De, M.; Rotello, V. M. *Curr. Opin. Chem. Biol.* **2005**, *9*, 639.
  - (28) Lucarini, M.; Franchi, P.; Pedulli, G. F.; Gentilini, C.; Polizzi, S.; Pengo, P.; Scrimin, P.; Pasquato, L. *J. Am. Chem. Soc.* **2005**, *127*, 16384.
  - (29) Chidsey, C. E. D. *Science* **1991**, *251*, 919.
  - (30) Gu, T.; Whitesides, J. K.; Fox, M. A. J. *Org. Chem.* **2004**, *69*, 4075.
  - (31) Centrone, A.; Penzo, E.; Sharma, M.; Myerson, J. W.; Jackson, A. M.; Marzari, N.; Stellacci, F. *Proc. Natl. Acad. Sci. U.S.A.* **2008**, *105*, 9886.
  - (32) Jackson, A. M.; Myerson, J. W.; Stellacci, F. *Nat. Mater.* **2004**, *3*, 330–336.
  - (33) Singh, C.; Ghorai, P. K.; Horsch, M. A.; Jackson, A. M.; Larson, A. M.; Stellacci, F.; Glotzer, S. C. *Phys. Rev. Lett.* **2007**, *99*, 226106.
  - (34) Jackson, A. M.; Hu, Y.; Silva, P.; Stellacci, F. *J. Am. Chem. Soc.* **2006**, *128*, 11135.
  - (35) Centrone, A.; Penzo, E.; Sharma, M.; Myerson, J. W.; Jackson, A. M.; Marzari, N.; Stellacci, F. *Proc. Natl. Acad. Sci.* **2008**, *105*, 9886.
  - (36) Zhao, X.; Leng, Y.; Cummings, P. T. *Langmuir* **2006**, *22*, 4116.
  - (37) Ghorai, P. K.; Glotzer, S. C. *J. Phys. Chem. C* **2007**, *111*, 15857.
  - (38) Allen, M. P.; Tildesley, D. J. *Computer Simulation of Liquids*; Clarendon Press: Oxford, U.K., 1987.
  - (39) Mar, W.; Klein, M. L. *Langmuir* **1994**, *10*, 188.
  - (40) Majumder, C.; Briere, T. M.; Mizuseki, H.; Yoshiyuki, J. *Chem. Phys.* **2002**, *117*, 2819.
  - (41) Forester, T. R.; Smith, W. *The DL-POLY-2.13*; CCLRC, Daresbury Laboratory: Warrington, England, 1985.
  - (42) Casagrande, C.; Veyssie, M. C. R. *Acad. Sci., Ser. II* **1988**, *306*, 1423.
  - (43) Velichko, Y. S.; de la Cruz, M. O. *J. Chem. Phys.* **2006**, *124*, 214705.
  - (44) S. M. overde, Y. S. V.; de la Cruz, M. O. *J. Chem. Phys.* **2006**, *144*, 144702.
  - (45) Velichko, Y. S.; de la Cruz, M. O. *Phys. Rev. E* **2005**, *72*, 041920.
  - (46) Vemparala, S.; karki, B. B.; Kalia, R. K.; Nakano, A.; Vashishtha, P. *J. Chem. Phys.* **2004**, *121*, 4323.